

Mechanism of curing behavior for CFRP compression molding under thermo-mechanical-chemical multi-field coupling

Jiu-ming Xie¹ , Xuejun Zhou¹, Jin Wu¹, Cong She², Chencheng Feng²

¹Tianjin Sino-German University of Applied Science, School of Mechanical Engineering, Jinnan District, Mingde Rd, Tianjin, China.

²Tianjin University of Technology, Binshui Xidao, Xiqing District, Tianjin, China.

e-mail: xiejiuming1983@163.com, zhouxuejun1978@163.com, wujin@tsguas.edu.cn, 13752119958@163.com, fengchencheng123@163.com

ABSTRACT

Curing is a critical process in the compression molding of carbon fiber reinforced polymer (CFRP). It directly bears on the quality of the molded products. Based on the curing theory of resin-based polymers, a thermo-mechanical-chemical multi-field coupling model for CFRP curing in the form of thermal-chemical subprocess, matrix flow-compaction sub-process and residual stress-deformation subprocess, and sets up its data exchange and mutual call relationship. Considering the thermal physics and chemical properties of composites change with temperatures, the authors introduced the thermal viscosity stiffness coefficient and took AS4/3501CFRP molded laminate as an example, and carried out a multi-field coupling simulation of the CFRP curing through compression molding, using the finite-element software COMSOL. The proposed model was proved correct through calculation of an example in the literature. Further, the CFRP curing mechanism was revealed through a detailed analysis on the evolution of temperature, curing degree, stress and strain of the CFRP curing through compression molding. The results show that the large internal temperature gradient during the compression molding of laminates is the main reason for the residual stress of materials and the deformation of laminate. Finally, an AS4/3501CFRP molded laminate was prepared, and its temperature field was monitored by fiber Bragg grating (FBG) transducers. The temperature evolution law of the material was consistent with the finite element simulation results, which demonstrate the correctness of the simulation.

Keywords: CFRP; Compression molding; Multi-field coupling; Mathematical model; curing behavior.

1. INTRODUCTION

Carbon fiber reinforced polymer (CFRP) is widely used in various fields, owing to its unique advantages like high specific strength and specific modulus, strong resistance to fatigue and corrosion, and excellent breakage safety and performance designability [1–3]. CFRP products can be molded through compression molding, autoclave wrapping, or pultrusion. Among them, compression molding is highly competitive in batch production of parts, especially large batch production, thanks to its low cost, high efficiency, as well as the small internal stress, limited buckling deformation, and good repeatability of its products [4,5]. The CFRP compression modeling is a multi-parameter coupling system. The curing of the CFRP is influenced by the coupling disturbances from multiple physical fields, process parameters, and material attributes, as well as the thermal-chemical reactions of the matrix [6–9]. As a result, it is very difficult to predict the curing deformation of the products.

Domestic and foreign scholars have studied CFRP curing extensively, and achieved fruitful results. In terms of numerical simulation, the early works mostly explore the distribution of internal temperatures and curing degrees, based on thermal-chemical models. Loos et al. [10] set up a one-dimensional (1D) model of the curing of an epoxy resin-prepreg polymer to describe the temperature field distribution and resin flow conditions. Cheung et al. [11] proposed a thermal-kinetic coupling model for polymers, and effectively forecasted the temperature and curing degree distributions during the molding process. In recent years, researchers of polymer curing started to investigate the multi-field coupling of thermal-chemical model and residual stress, and predict the evolution of composite deformation and residual stress. Bogetti et al. [12] combined with curing simulation analysis with incremental laminate theory to examine the relationships between temperature, curing degree gradient, residual stress, and curing deformation. White et al. [13] adopted implicit finite-element difference

to project the distributions of temperatures and curing degrees through the curing process, and established a two-dimensional (2D) finite-element model to predict the residual stress. Ma Yunrong et al. [14] constructed a curve coordinate system based on steady flow line equations, and successfully predicted the variation in the distribution of temperatures, curing degrees, and internal stresses of stressed-skin plates through the curing process. The existing constitutive models for curing deformation mainly fall into linear elastic model and viscoelastic model. The latter is the mainstream tool among researchers. Li et al. [15] built a three-dimensional (3D) finite-element model for the curing process, and tentatively solved the multi-physical field coupling of thermal-chemical model and viscoelastic constitutive model. Considering the thermal-chemical effect during polymer curing, Min Rong et al. [16] predicted curing deformation of polymers, in the light of the viscoelastic features of the resin matrix. The author [17] took account of the influence of temperature on initial stiffness and equilibrium stiffness, established the anisotropic constitutive model of the curing process, and effectively forecasted the temperature field and curing field through the curing process.

During the compression molding of CFRP, the material attributes change constantly with temperatures and pressures. To better simulate the curing process under compression molding, this paper adopts the material attributes related to temperature to examine the curing process of CFRP under compression molding under the thermal-force-chemical field coupling, and explore the mechanism of CFRP compression molding. The research results lay theoretical groundworks and provide scientific bases for understanding the mechanism of CFRP compression molding, gaining insights to the shared nature of compression molding of various carbon fiber polymers, and extending the application scope of these products, especially various high-quality carbon fiber polymer products.

2. MODELING

According to the variation of matrix state, The Gel point and glass transition temperature of the Matrix is taken as the dividing principle, the curing process of CFRP compression molding was divided into three sub-processes for modeling: the thermal-chemical sub-process, the matrix flow-compaction sub-process, and the residual stress-deformation sub-process.

2.1. Model of thermal-chemical subprocess

During the curing of CFRP compression molding, the external heat source transmits heat to the inside of the material via the material surface. Meanwhile, the matrix curing releases energy [18]. This process can be described as a non-steady thermal conduction problem of a nonlinear internal heat source.

According to Fourier's law of thermal conduction and energy balance equation, the thermal conduction of matrix curing can be described by a 3D thermal conduction control equation, including a nonlinear internal heat source,

$$\rho C_p \frac{\partial T}{\partial t} = \frac{\partial}{\partial x} \left(k_x + \frac{\partial T}{\partial x} \right) + \frac{\partial}{\partial y} \left(k_y + \frac{\partial T}{\partial y} \right) + \frac{\partial}{\partial z} \left(k_z + \frac{\partial T}{\partial z} \right) + \frac{\partial Q}{\partial t} \quad (1)$$

where, ρ , C_p , T , and t are density, specific heat, temperature, and time, respectively; k_x , k_y , and k_z are thermal conduction coefficients in the global coordinate system of the material; Q is the energy released by the basic curing reaction; $\frac{\partial Q}{\partial t}$ is the heat generation rate, i.e., the heat generated by the chemical reaction per unit of time.

$$\frac{\partial Q}{\partial t} = \rho_r (1 - v_f) H_R \frac{d\alpha}{dt} \quad (2)$$

where, ρ_r is the fiber volume content; H_R is the total heat released through the chemical reaction by a unit mass of matrix; α is the curing degree, i.e., the degree of curing crosslinking reaction, which is the ratio of the current heat release to the total heat release; $\frac{d\alpha}{dt}$ is the curing reaction rate, i.e., the curing degree as a function of temperature in the phenomenological curing kinetics.

$$\frac{d\alpha}{dt} = g(T, \alpha) = k(T) f(\alpha) \quad (3)$$

where, $f(\alpha)$ is a function with curing degree as the independent variable; $k(T)$ is the constant reaction rate, which can be depicted as an exponential function of temperature satisfying the Arrhenius formula:

$$k(T) = A \exp\left(-\frac{\Delta E}{RT}\right) \quad (4)$$

where, A is the frequency factor; ΔE is the activation energy of viscous flow; R is the universal gas constant; T is the absolute temperature.

The specific forms and values of $f(\alpha)$, A and ΔE can be measured through differential scanning calorimetry (DSC)[19].

The curing degree can be calculated by:

$$\alpha(t) = \int_0^t \frac{d\alpha}{dt} \quad (5)$$

The boundary condition of the thermal conduction model can be expressed as

$$K_{eff} \frac{\partial T}{\partial n} + h_{eff} (T_s - T_m) = 0 \quad (6)$$

where, T_s and T_m are the surface temperature and heating temperature of the polymer, respectively; K_{eff} and h_{eff} are the equivalent thermal conduction coefficient and the equivalent thermal convection coefficient of the polymer surface, respectively.

The boundary conditions of the heat conduction problems of CFRP in the compression molding process include the forced boundary conditions, the adiabatic boundary conditions and the natural convection boundary conditions. Corresponding equation (7–9) respectively.

$$T = \bar{T} \quad (7)$$

$$k_x \frac{\partial T}{\partial x} n_x + k_y \frac{\partial T}{\partial y} n_y + k_z \frac{\partial T}{\partial z} n_z = q \quad (8)$$

$$k_x \frac{\partial T}{\partial x} n_x + k_y \frac{\partial T}{\partial y} n_y + k_z \frac{\partial T}{\partial z} n_z = h(T_\alpha - T) \quad (9)$$

Where, h is Convective heat transfer Coefficient and T_α is adiabatic wall temperature.

2.2. Model of matrix flow-compaction sub-process

According to Guski's "Extruding sponge" model, the external pressure is shared by the fiber and the resin. The Resin Matrix flows along the fiber direction and perpendicular to the fiber direction in the fiber bed after melting, the prepreg laminates can be regarded as a porous medium with nonlinear elastic deformation properties filled with viscous fluid, and the flow of the excess resin out of the composite can be regarded as a flow problem of the porous medium in saturated state, the Matrix flow impregnation equation is described by Darcy's Theorem as:

$$(\mathbf{v}) = -\frac{K}{\eta} (\nabla P) \quad (10)$$

where, \mathbf{v} is the fluid velocity, P is the pressure, η is the fluid viscosity, and K is the permeability.

Considering that the liquid resin in the prepreg laminates is incompressible, and taking into account the volume change of the matrix flowing into the micro-element per unit time, the continuity equation of resin flow can be expressed as:

$$\frac{\partial v_x}{\partial x} + \frac{\partial v_y}{\partial y} + \frac{\partial v_z}{\partial z} + \Delta v = \frac{\partial}{\partial t} \left(\frac{\partial v_x}{\partial x} + \frac{\partial v_y}{\partial y} + \frac{\partial v_z}{\partial z} \right) \quad (11)$$

where, v_x , v_y and v_z are the micro-flow speeds of the matrix in x , y , and z directions, respectively; Δv is the volume change of the matrix through melting under pressure; u , v , and w are the displacements of the reinforced fibers in x , y , and z directions, respectively.

The Matrix percolates between the carbon fibers and is impregnated, at which point Darcy's law can be expressed as:

$$\begin{cases} v_x = -\frac{s_x}{\mu} \frac{\partial p_r}{\partial x} \\ v_y = -\frac{s_y}{\mu} \frac{\partial p_r}{\partial y} \\ v_z = -\frac{s_z}{\mu} \frac{\partial p_r}{\partial z} \end{cases} \quad (12)$$

where, μ is the viscosity of resin and p_r is the pressure of resin.

According to formulas (12), the continuity equation of resin flow can be expressed as:

$$\frac{\partial}{\partial x} \left(\frac{s_x}{\mu} \frac{\partial p_r}{\partial x} \right) + \frac{\partial}{\partial y} \left(\frac{s_y}{\mu} \frac{\partial p_r}{\partial y} \right) + \frac{\partial}{\partial z} \left(\frac{s_z}{\mu} \frac{\partial p_r}{\partial z} \right) - \frac{\partial}{\partial t} \left(\frac{\partial v_x}{\partial x} + \frac{\partial v_y}{\partial y} + \frac{\partial v_z}{\partial z} \right) + \Delta v = 0 \quad (13)$$

The permeability rate is related to the volume fraction, diameter, and structure of the fibers. It is generally described by the following empirical formula (14):

$$K_{ij} = \frac{r_f^2}{4K_0} \cdot \frac{(1-V_f)^2}{V_f^2} \quad (14)$$

where, r_f is the radius of the fibers; K_0 is the Kozeny constant, which changes with the fiber structure and matrix flow direction.

Tensor's equation for permeability can be expressed as:

$$K_x \frac{\partial^2 P}{\partial x^2} + K_y \frac{\partial^2 P}{\partial y^2} + K_z \frac{\partial^2 P}{\partial z^2} = 0 \quad (15)$$

where, K_x , K_y and K_z is the main permeability in x , y and z directions;

In the compaction phase, it is assumed that the fibers are incompressible and stretchable, and that the resin flows between the fibers and is saturated. At this point, the mechanical equilibrium equation can be expressed by the criterion of effective stress as:

$$\sigma = \bar{\sigma} + p_r \quad (16)$$

where, σ is external pressure and $\bar{\sigma}$ effective stress of fiber bed.

In this case, the total stress is composed of the effective stress of the fibers, and resin pressure:

$$\sigma_{ij} = \sigma_{ij}^f - \delta_{ij} P_r \quad (17)$$

where, σ_{ij}^f is the effective stress of the fibers; δ_{ij} is the Kronecker delta; P_r is the resin pressure.

At this time, the compression equation of the polymer can be expressed as:

$$\frac{K_{xx}}{V_f} \cdot \frac{\partial^2 P_r}{\partial x^2} + \frac{K_{yy}}{V_f} \cdot \frac{\partial^2 P_r}{\partial y^2} + \frac{1}{V_0} \cdot \frac{\partial}{\partial z} \left(V_f K_{zz} \frac{\partial P_r}{\partial z} \right) = \mu \frac{\partial}{\partial t} \left(\frac{1-V_f}{V_f} \right) \quad (18)$$

where, V_0 is the zero-load fiber volume fraction of fibers; V_f is the volume fraction of the fibers;

During matrix seepage, the thickness h of the CFRP laminate changes by:

$$-\frac{d(hS)}{dt} = \frac{KP_r}{\mu h} \quad (19)$$

where, S is the spreading area of the polymer.

2.3. Model of residual stress-deformation subprocess

Residual stress generated during the curing process of resin matrix composites will lead to the curing deformation of its components, which is the root cause of problems such as warping, delamination, and cracking of molded parts. The residual stress mainly comes from two aspects: one is the thermal stress caused by the mismatch between the thermal expansion coefficients of the matrix resin and the reinforcing fiber during the curing temperature change process; the other is the curing shrinkage stress generated by the curing cross-linking reaction of the matrix resin.

The expression of residual stress in cured composites can be described by:

$$\sigma_{ij} = C_{ij} \left[\varepsilon_{ij} - (\varepsilon_{ij}^t + \varepsilon_{ij}^c) \right] \quad (20)$$

Where, C_{ij} is the instantaneous stiffness matrix component of composite material, which can be obtained by using the engineering elastic parameters related to resin and fiber through the mechanical theory of composite material; σ_{ij} is the internal stress component; ε_{ij} is the total strain component; ε_{ij}^t and ε_{ij}^c are the thermal strain and chemical shrinkage strain components of composites, respectively.

The elastic modulus of the matrix changes dramatically as curing progresses, further resulting in the change in C_{ij} . The elastic modulus is related to the degree of curing and can be described by:

$$\begin{cases} E_r = E_r^0 & \alpha < \alpha_g \\ E_r = (1-\alpha)E_r^0 + \alpha_m E_r^\infty & \alpha \geq \alpha_g \end{cases} \quad (21)$$

$$\alpha_m = \frac{\alpha - \alpha_g}{1 - \alpha_g} \quad (22)$$

Where, E_r^0 and E_r^∞ are the elastic modulus of the matrix uncured and fully cured, respectively; α_g is the degree of cure for matrix gel point.

The thermal strain is primarily induced by the thermal expansion and cold contraction effect of the temperature variation through the curing process. It can be described by:

$$\varepsilon^t = \alpha_i \Delta T \quad (i = x, y, z) \quad (23)$$

where, α_i is the equivalent thermal expansion coefficient of polymer in three directions.

The CFRP is an anisotropic material. It is assumed that the x direction is the fiber direction, and y - z is an isotropic surface. Then, the thermal expansion coefficients of different directions can be expressed as:

$$\alpha_x = \frac{\alpha_{xf} E_{xf} V_f + \alpha_m E_m V_m}{E_{xf} V_f + E_m V_m} \quad (24)$$

$$\begin{aligned} \alpha_y = \alpha_z = & (\alpha_{yf} + \nu_{xyf} \alpha_{xf}) V_f + (\alpha_m + \nu_m \alpha_m) (1 - V_f) \\ & - \left[\nu_{xyf} V_f + \nu_m (1 - V_f) \right] \frac{\alpha_{xf} E_{xf} V_f + \alpha_m E_m (1 - V_f)}{E_{xf} V_f + E_m (1 - V_f)} \end{aligned} \quad (25)$$

where, the subscripts m and f are matrix and reinforced fibers, respectively; α_{yf} and α_{yf} are thermal expansion coefficients parallel to or perpendicular to fiber direction, respectively; E_{xf} and V_{xyf} are the Poisson's ratios of the fibers in the fiber direction and on the x - y plane, respectively; E_m , ν_m , and α_m are the elastic model, Poisson's ratio, and thermal expansion coefficient of the matrix, respectively.

Suppose the matrix contracts by the same amount in all directions. Then, the chemical contraction strain of the matrix can be expressed as:

$$\varepsilon_m^c = \sqrt[3]{1 + \Delta v} - 1 \tag{26}$$

The volume change rate Δv of the matrix is associated with the curing degree and the total volume contraction V_{sh} after full curing:

$$\Delta v = \Delta \alpha \cdot V_{sh} \tag{27}$$

The chemical shrinkage strain in the principal direction is expressed as::

$$\varepsilon_x^c = \varepsilon_{xf}^c \frac{E_{xf} V_f}{E_{xf} V_f + E_m V_m} \tag{28}$$

$$\begin{aligned} \varepsilon_y^c = \varepsilon_z^c = & (\varepsilon_{yf} + \nu_{xyf} \varepsilon_{xf}) V_f + (\varepsilon_m + \nu_m \varepsilon_m) (1 - V_f) \\ & - \left[\nu_{xyf} V_f + \nu_m (1 - V_f) \right] \frac{\varepsilon_{xf} E_{xf} V_f + \varepsilon_m E_m (1 - V_f)}{E_{xf} V_f + E_m (1 - V_f)} \end{aligned} \tag{29}$$

2.4. Data relationship between models

During CFRP compression molding, the physical and chemical phenomena of different sub-processes may occur simultaneously, and impact each other. The impacts are manifested by the data exchange between sub-process models shows as Figure 1.

During compression molding of CFRP, the matrix gradually transitions to a molten state and a liquid state caused by the external heat source and the curing reaction exothermic. When the matrix is in a liquid state,

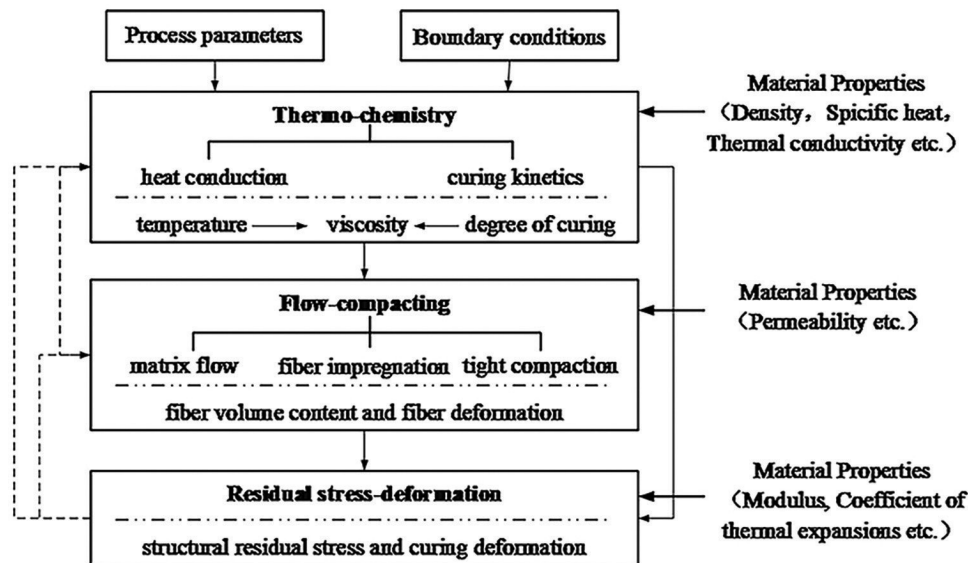


Figure 1: Data exchange between sub-processes.

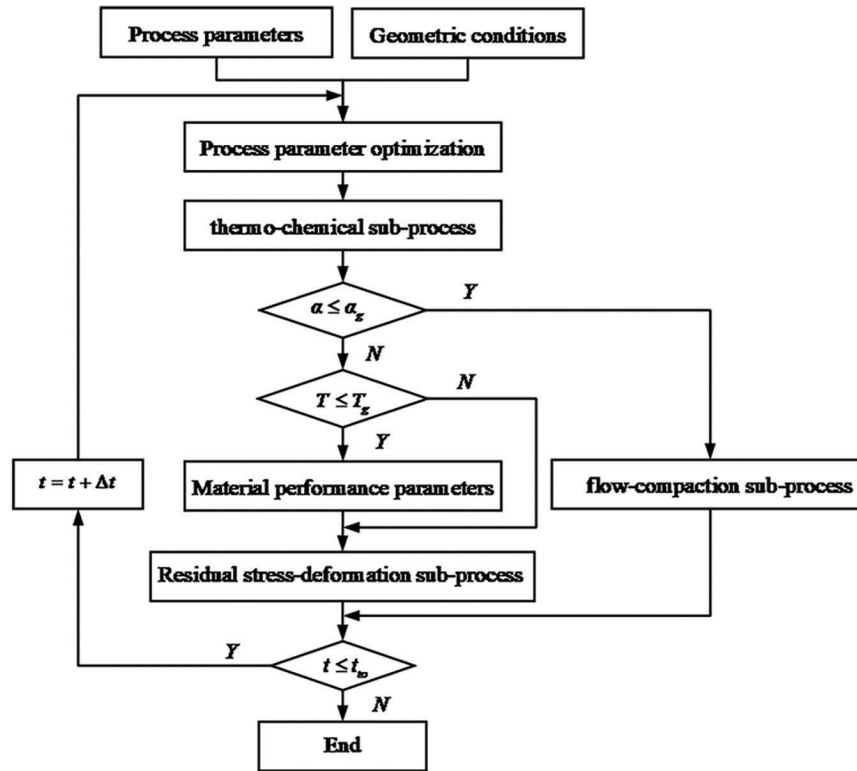


Figure 2: Calling relationships between sub-processes at different moments.

the fibers will not deform, nor produce any residual stress. After gelation, the matrix sees a gradual increase of modulus. The residual stress produced by the curing shrinkage is released, due to the viscoelastic effect of the resin. Once the matrix enters the glassy state, the residual stress produced by the curing shrinkage would increase linearly with the growing curing degree. Therefore, the gel point α_g and the glass transition temperature T_g were taken as judgement criteria. Figure 2 shows the calling relationships between sub-processes at different moments.

3. SIMULATION

The example in Kim's work [20] has been verified repeatedly through simulations and experiments, and taken as a reference. Taking the AS4/3501-6 series polymer produced by American company Hercules as an example, this paper simulates the compression molding process under thermal-force-chemical multi-field coupling, with the aim to demonstrate the correctness of our model.

3.1. CFRP material attributes

The material attributes of the matrix and the reinforced fibers are needed to simulate the curing process of the CFRP. Based on the thermal conduction equations (14–20) in the mathematical models, the thermal physical parameters of the matrix and the reinforced fibers are listed in Table 1.

The curing kinetic equation of the 3501-6 epoxy resin matrix can be described by a piecewise function:

$$\begin{cases} \frac{d\alpha}{dt} = (k_1 + k_2\alpha)(1-\alpha)(0.47-\alpha) & \alpha \leq 0.3 \\ \frac{d\alpha}{dt} = k_3(1-\alpha) & \alpha > 0.3 \end{cases} \quad (30)$$

where, the reaction rate can be described by Arrhenius equation:

$$k_i(T) = A_i \exp\left(-\frac{E_{ai}}{RT}\right) \quad i = 1, 2, 3 \quad (31)$$

Table 1: Thermal physical parameters of the matrix and the reinforced fibers.

PARAMETERS	SYMBOLS	EXPRESSIONS OR VALUES	UNITS
Fiber density	ρ_f	1790	$\text{kg}\cdot\text{m}^{-3}$
Matrix density	ρ_r	$\begin{cases} 90\alpha + 1232 & (\alpha \leq 0.45) \\ 1272 & (\alpha > 0.45) \end{cases}$	$\text{kg}\cdot\text{m}^{-3}$
Specific heat of fibers	C_p^f	$1390 + 4.5 \times 10^{-3}T$	$\text{J}\cdot\text{kg}\cdot\text{K}^{-1}$
Specific heat of matrix	C_p^r	$4184(0.468 + 5.975 \times 10^{-4}T - 0.141\alpha)$	$\text{J}\cdot\text{kg}\cdot\text{K}^{-1}$
Thermal conduction coefficient of fibers	K_f	$0.742 + 9.02 \times 10^{-4}T$	$\text{W}/(\text{m}\cdot\text{K})$
Thermal conduction coefficient of matrix	K_r	$0.04184[3.85 + (0.035T - 0.141\alpha)]$	$\text{W}/(\text{m}\cdot\text{K})$
Heat release of matrix after fully curing	H_r	3.078×105	J/kg

The reference values of the expression are given by [21].

For the residual stress-deformation sub-process of CFRP compression molding, the mechanical performance parameters of AS4 carbon fibers and 3501-6 resin matrix are given by [22].

Since initial stiffness and equilibrium stiffness of the material are related to material temperature, the temperature-related thermal stiffness coefficient was defined and added to the viscoelastic model of the material. Referring to Kim's test and data processing methods [23], the thermal elastic stiffness coefficient can be described by an exponential function:

$$f = 1.0827 \exp(-0.00272T) \tag{32}$$

3.2. Finite-element model

The fiber volume fraction of the prepreg is 50%. With the single layer thickness of 6.35mm, the prepreg was laid in the manner of $[0^\circ/90^\circ/90^\circ/0^\circ]$. Then, in order to ensure that the model is consistent with the literature example, a model was established with the size $10.16 \times 10.16 \times 2.54 \text{cm}^3$. Considering the geometric and boundary symmetry of the laminate, a $1/4$ model was set up, and divided into 1,600 hexagonal grids (Figure 3).

3.3. Curing parameters

The curing parameters were determined according to the prepreg performance (Figure 4).

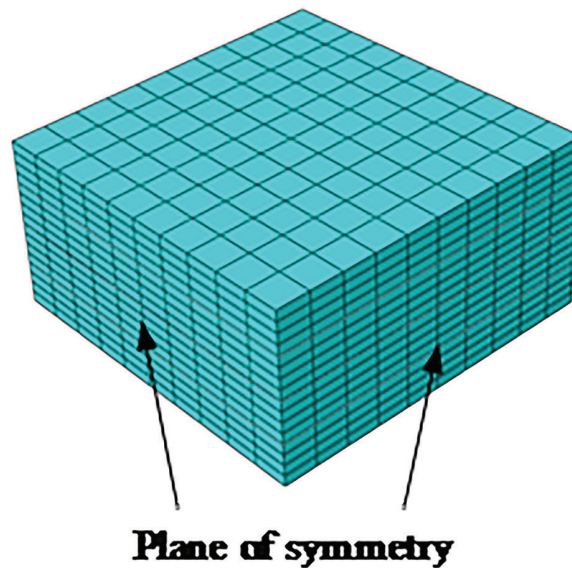


Figure 3: Finite-element model and grid division.

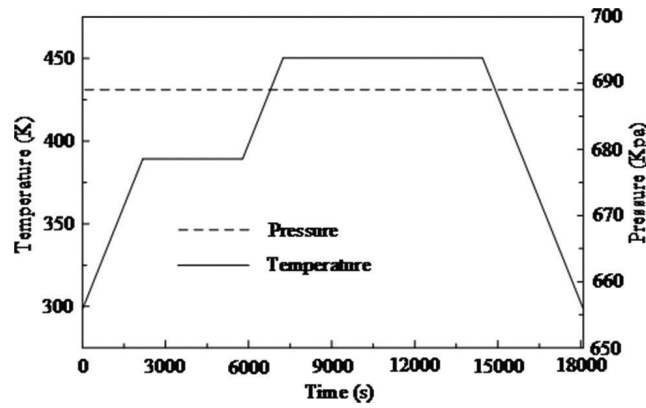


Figure 4: Curing process of the CFRP.

The temperature was initialized at room temperature (298.15K), and heated up to 389.15K at 2.5K/min. The temperature was then held for 1h. After that, the temperature was increased to 450.15k at the same rate. After a 2h holding period, the temperature was reduced at -2.5K/min to 298.15K. The pressure load of 689kPa was applied on the upper surface and the asymmetric surfaces around the laminate. The bottom of the laminate was supported by rollers.

3.4. Temperature and curing degree

Figures 5 and 6 show the variation of the temperature and curing degree at the center of the laminate with time, through the curing process of the polymer, respectively. It can be seen that the simulation results basically agree with the selected example, reflecting the correctness of our thermal-chemical model.

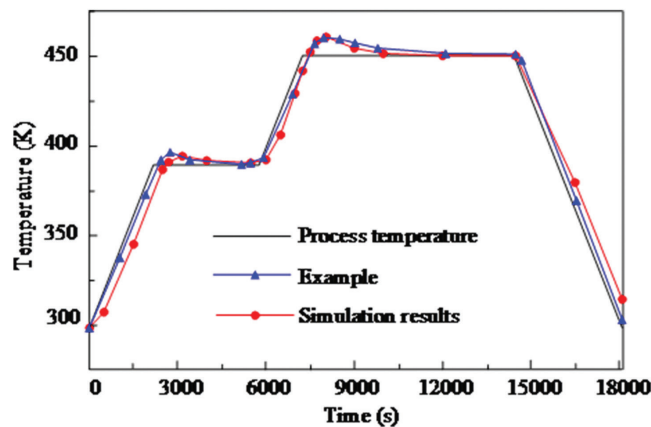


Figure 5: Temperature variation at the center of the laminate.

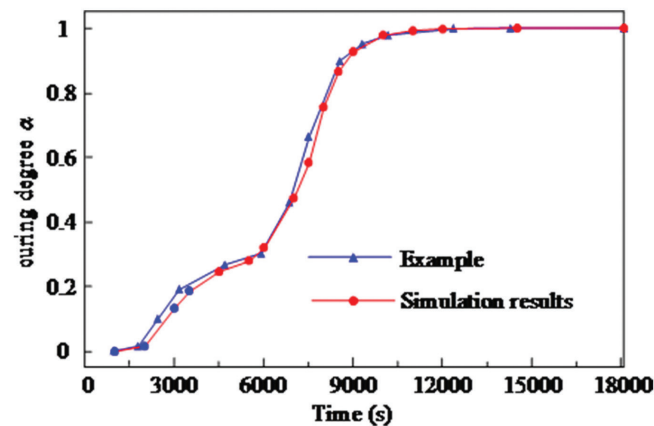


Figure 6: Curing degree variation at the center of the laminate.

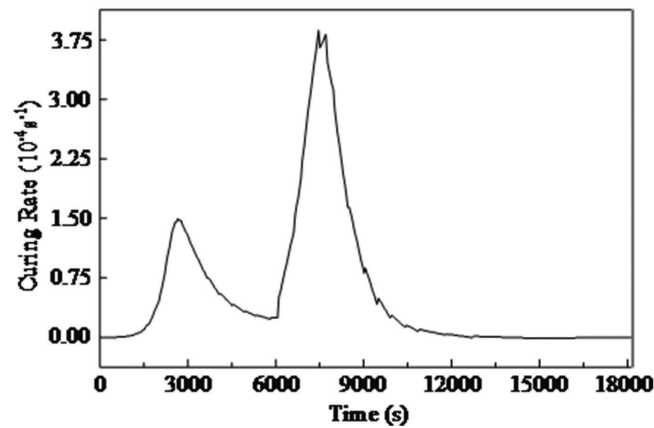


Figure 7: Curing rate curve at the center of the laminate.

In Figure 5, the center point temperature peaked at 393K and 460K within 3,150s and 8,050s after the start of the two temperature holding periods, respectively. Combined with the center point curing rate curves in Figure 7, it can be learned that the peak time of center point temperature corresponded with the peak time of the curing rate. Hence, the central point curing degree undergoes a rapid growth, i.e., the resin is subject to an intense curing reaction, releasing lots of heat through chemical reactions. Given the poor thermal conductivity of the polymer, and the thickness of the laminate, the heat would accumulate in the central area in a short time, causing the temperature to soar. The center point curing rate reached 1 at about 12,000s in the second temperature holding period, suggesting the basic completion of the curing process.

Figure 8 shows the cloud map of the temperature field distribution at the time slices of 2,000, 3,150, 7,000, 8,050, 12,000, and 15,000s. The cloud map is clearly in line with the above conclusions.

3.5. Stress and strain

Figure 9 shows the curve of the positive interlaminar stress at the center point through the curing process. It can be seen that the modeling result basically agrees with the curve change in the example. Hence, the proposed residual stress-deformation model is correct.

In Figure 9, during the initial period of the curing process (before 7,000s), the curing degree of 3501-6 was lower than that at the gel point of the resin. During this period, the resin was a viscous flow, and the positive interlaminar stress was almost zero. Soon, the resin completed gelation and glass transition, and the positive interlaminar stress rose steadily. The elastic modulus of the resin quickly rose from 0, and tended to be stable. At this time, the curing reaction was complete. Subsequently, the interlaminar stress at the center point increased significantly, as the positive interlaminar stress arrived at 36MPa. This is because the cooling creates a large temperature gradient inside the material. The resulting thermal effect leads to a large residual stress within the material. This is a major reason for the lamination and buckling failures of the laminate. As for the cooling period, this paper introduces the matrix flow-compaction model, which causes a slight deviation from the example. Overall, our model captures the stress change through the polymer curing very realistically.

It should be noted that, matrix flow-compaction sub-process is an intermediate process of the three sub-processes, and there is no quantitative analysis in the literature examples. During the simulation of CFRP compression molding, the reaction matrix flow-compaction sub-process is generally indirect through the analysis of curing degree, stress and strain [23]. It is believed that the matrix flow-compaction model is correct form Figure 5 and 9.

Figure 10 shows the curves of thermal strain and chemical contraction strain in the thickness direction at the center point. Obviously, the thermal strains in that direction changed basically the same as the temperature did. During the intense exothermal period of the curing process, two thermal strain peaks appeared. The two apparent change phases of chemical contraction strain were the same as those of the curing crosslinking reaction. In general, the thermal expansion effect was far more significant than chemical contraction in the early phase. With the progression of the curing reaction, the chemical contraction strain gained dominance.

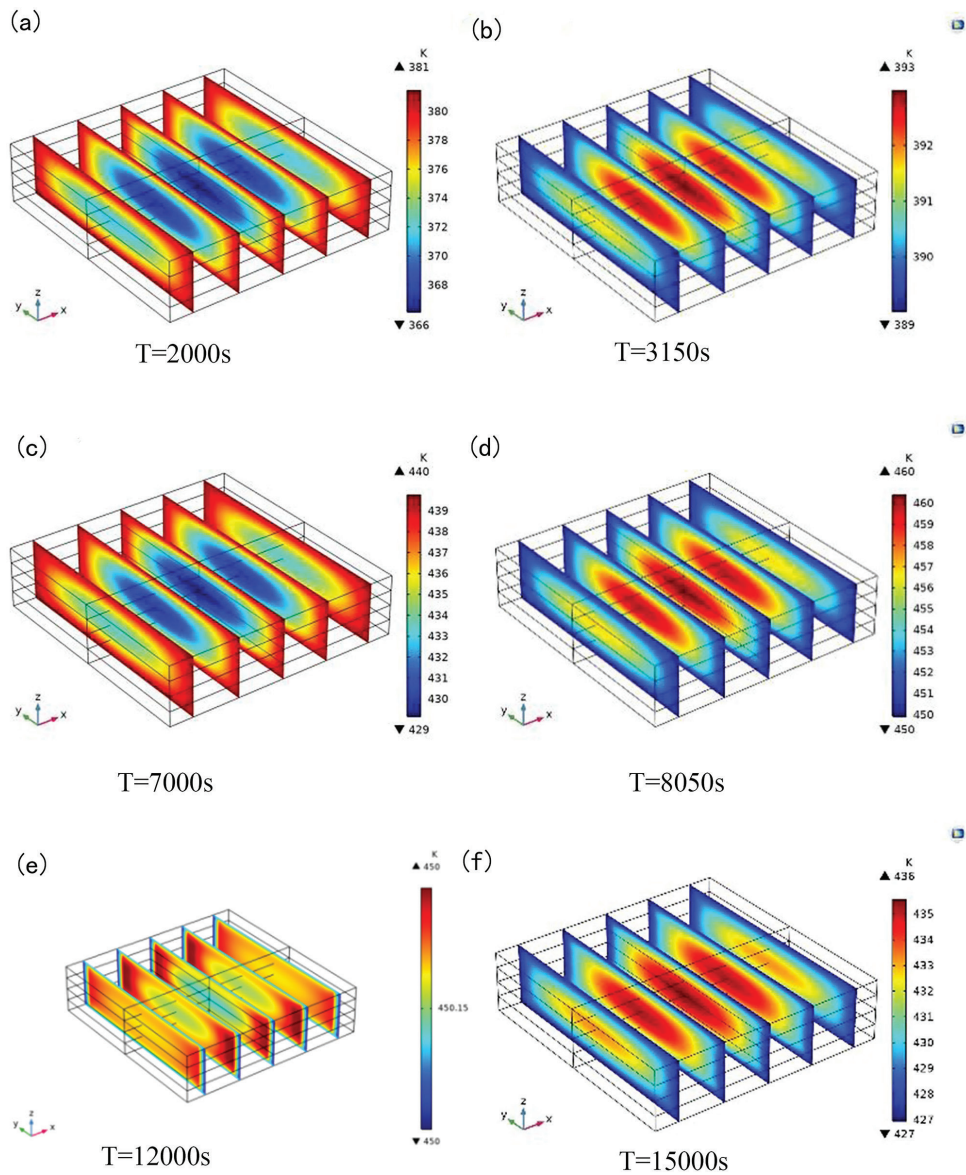


Figure 8: Cloud map of temperature field distribution through the curing process: (a) T (Time) = 2000 s, (b) T = 3150 s, (c) T = 7000 s, (d) T = 8050 s, (e) T = 12000 s, (f) T = 15000 s.

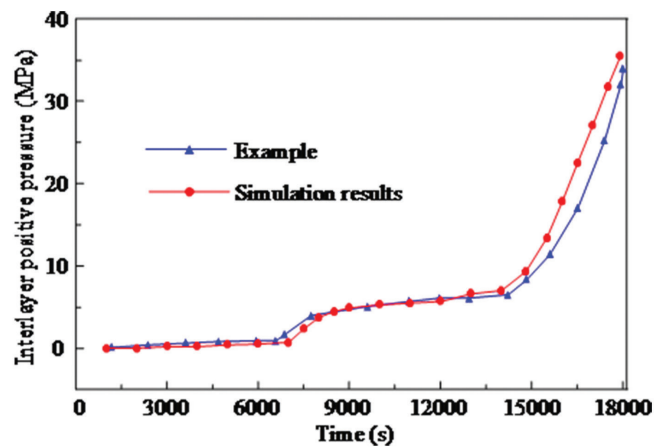


Figure 9: Positive interlaminar stress at the center point of the laminate.

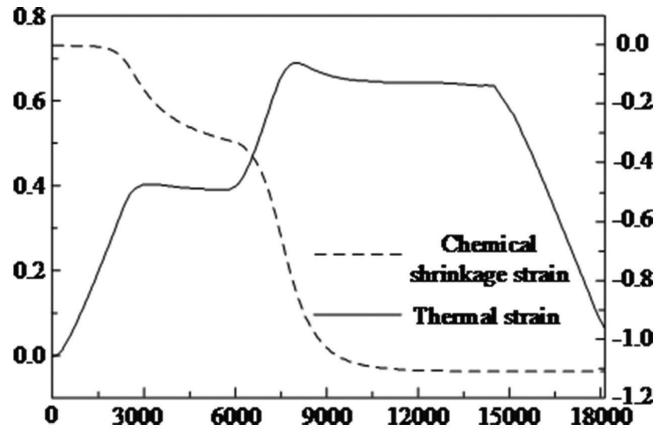


Figure 10: Thermal strain and chemical contraction strain in the thickness direction at the center point.

4. EXPERIMENTAL ANALYSIS

4.1. Materials and instruments

Our experiments use AS4/3501 prepreg produced by Hexcel Corporation. The single layer thickness and laying method are the same as the simulation. Table 2 lists the instruments adopted for the experiments.

4.2. Experimental process

According to the model of the press, the size of the prepreg was 500mm × 500mm. In order to ensure the comparability and consistency of the experimental and simulation results, the thickness is consistent with the simulation model. During the stacking of prepregs, the FBG transducers (FBG-Ts) were embedded at the center positions of the second and third layers. Since the laminate is thin, multiple tests with pre-embedded transducers failed. In future, thick laminate will be adopted for strain monitoring.

During compression molding, release agent should be painted on the mold. To prevent the spillover of the resin from the prepreg, a return box was configured for the mold. Oil heating and cooling were selected for the system. The processing was carried out with the process parameters of the previous simulation. The procedure of the experiments is illustrated in Figure 11.

Table 2: Instruments.

INSTRUMENT	MANUFACTURER	REMARK
Compressor-Tianjin Sino-German University of Applied Sciences Platform Equipment	Tianjin Tianduan Press Co., Ltd.	Size: 500mm × 500mm
SI 255 Fiber optic sensing interrogator	Micron Optics	Sampling frequency: 10Hz; wavelength accuracy: 1pm
Fiber Bragg grating (FBG) transducer	Nanjing KJT Electric Co., Ltd.	Temperature sensitivity: 10.8pm/°C; strain sensitivity: 1.2pm/με
Channel expander	Cavono, Inc.	

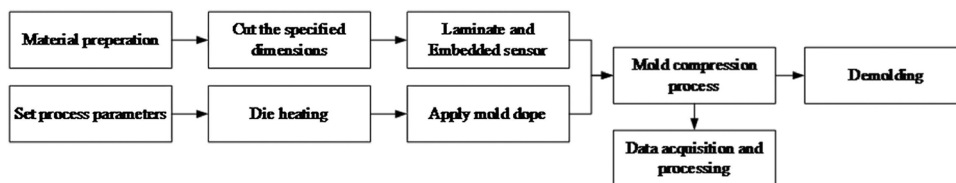


Figure 11: Procedure of compression molding experiments.



Figure 12: Procedure of compression molding experiments.



Figure 13: The CFRP laminates.

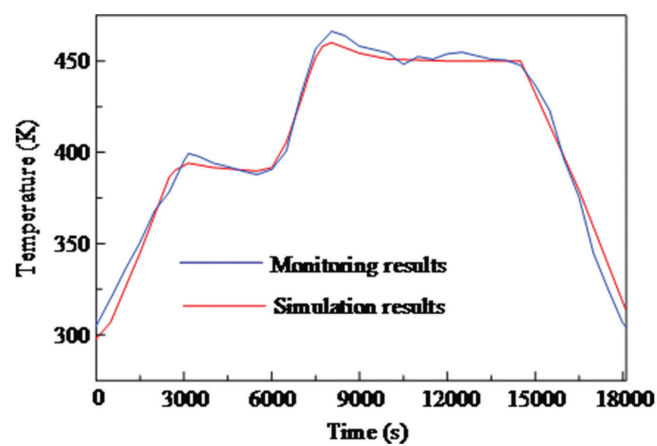


Figure 14: Change law of material temperature.

The experimental process is shown in Figure 12.

The CFRP laminates prepared for relevant performance experiments after cutting is shown in Figure 13.

4.3. Temperature monitoring

Figure 14 records the change law of material temperature monitored by FBG-Ts.

As shown in Figure 14, the change law of material temperature monitored by FBG-Ts was largely consistent with the finite-element simulation results. This again confirms the correctness of our constitutive models and finite-element simulation. At the initial moment (0s), the monitored temperature was slightly higher than the simulated temperature. The main reason is that the prepreg is preheated during the laying process, aiming to better fix the FBG-Ts. The temperature is also pushed up by the exothermic reaction during the preheating. In the first temperature holding period, the monitored temperature was above the simulated temperature. This is because the oil temperature needs a while to stabilize, when the control system is under heat preservation, after the mold is heated. Due to the heat preservation, the mold becomes a bit hotter. The same was observed in the second temperature holding period. In addition, the second period witnessed significant temperature variations. There are two causes of the variations. Firstly, the delay of oil temperature causes the control system to adjust the mold temperature continuously. More importantly, the mold heating, thermal-chemical reaction, and matrix curing work together to affect the temperature. During the cooling stage, the monitored temperature eventually fell below the simulated temperature, owing to the delay of oil temperature.

5. CONCLUSIONS

In this Paper, the process of CFRP compression molding was divided into three sub-processes: the thermal-chemical sub-process, the matrix flow-compaction sub-process, and the residual stress-deformation sub-process. Then, the authors set up a constitutive model of each sub-process, and built the data relationships and the calling relationships between sub-processes. Considering the relationship between material attributes and temperature, described the elastic stiffness with an exponential function, and simulated the CFRP compression molding under thermal-force-chemical coupling, and the results demonstrate the correctness of our constitutive models. The temperature field, curing degree field, stress field, and strain field were analyzed through the CFRP compression molding, and the mechanism of compression molding was explored. FBG-Ts were adopted to monitoring the temperature change during compression molding, and the monitoring results confirm the correctness of our constitutive models and simulation.

6. ACKNOWLEDGMENTS

The research of this paper is made possible by the generous support from Tianjin Sino-German University of Applied Sciences and Tianjin University and Xi'an Jiaotong University.

7. BIBLIOGRAPHY

- [1] Rana, S., Figueiro, R., *Advanced Composite Materials for Aerospace Engineering*. Cambridge: Elsevier, 2016.
- [2] Straznický, P.V., Laliberté, J.F., Poon, C., *et al.*, “Applications of Fiber-Metal Laminates”, *Polymer Composites*, v. 21, n. 4, pp. 558–567, 2010.
- [3] Du, S., “Advanced composite materials and aerospace engineering”, *Fuhe Cailiao Xuebao/Acta Materiae Compositae Sinica*, v. 24, n. 1, pp. 1–12, 2007.
- [4] Pramanik, A., Basak, A.K., Dong, Y., *et al.*, “Joining of carbon fiber reinforced polymer (CFRP) composites and aluminium alloys-A review”, *Composites Part A Applied Science & Manufacturing*, v. 101, pp. 1–29, 2017.
- [5] Gibson, R.F., *Principles of Composite Material Mechanics*. Boca Raton: CRC Press, 2011.
- [6] Molchanov, E.S., Yudin, V.E., Kydraliev, K.A., *et al.*, “Comparison of the thermomechanical characteristics of porous carbon fabric-based composites for orthopaedic applications”, *Mechanics of Composite Materials*, v. 48, n. 3, pp. 343–350, 2012.
- [7] Christensen, R., *Theory of Viscoelasticity: an introduction*. New York: Dover Publications, 1982.
- [8] Soomgin, P., Minkgang, S., “Carbon Fiber-Reinforced Polymer Composites: Preparation, Properties, and Applications”, *Polymer Composites*, v. 1, pp. 135–183, 2012.
- [9] Kumar, A.P., Dirgantara, T., Krishna, P.V., *Advances in Lightweight Materials and Structures*. Switzerland: Springer, 2020.
- [10] Loos, A.C., Springer, G.S., “Curing of Epoxy Matrix Composites”, *Journal of Composite Materials*, v. 7, n. 2, pp. 135–169, 1983.
- [11] Cheung, A., Yu, Y., Pochiraju, K., “Three-dimensional finite element simulation of curing of polymer composites”, *Finite Elements in Analysis & Design*, v. 40, n. 8, pp. 895–912, 2004.

- [12] Bogetti, T.A., Gillespie, J.W., “Process-Induced Stress and Deformation in Thick-Section Thermoset Composite Laminates”, *Journal of Composite Materials*, v. 26, n. 5, pp. 626–660, 1992.
- [13] White, S.R., Kim, Y.K., “Process-induced residual stress analysis of AS4/3501–6 composite material”, *Mechanics of Composite Materials & Structures*, v. 5, n. 2, pp. 153–186, 1998.
- [14] Msallem, Y.A., Jacquemin, F., Poitou, A., “Residual stresses formation during the manufacturing process of epoxy matrix composites: resin yield stress and anisotropic chemical shrinkage”, *International Journal of Material Forming*, v. 3, n. 2, pp. 1363–1372, 2010.
- [15] Yunrong, M.A., Jilin, H.E., Dong, L.I., *et al.*, “Numerical simulation of curing deformation of resin matrix composite curved structure”, *Acta Materiae Compositae Sinica*, v. 684, pp. 145–153, 2015.
- [16] Min, R., Yuan, Z., Wang, Y., *et al.*, “Numerical simulation for curing deformation of resin matrix thermosetting composite using viscoelastic constitutive model”, *Acta Materiae Compositae Sinica*, v. 34, n. 10, pp. 2254–2262, 2017.
- [17] Xie, J., Wang, S., Cui, Z., *et al.*, “Research on Anisotropic Viscoelastic Constitutive Model of Compression Molding for CFRP”, *Materials*, v. 13, n. 10, 2277, 2020.
- [18] Bártolo, J.P., *Theoretical and Modeling Aspects of Curing Reactions*. Boston: Springer, 2011.
- [19] Ramis, X., Cadenato, A., Salla, J.M., “Curing of a thermosetting powder coating by means of DMTA, TMA and DSC”, *Polymer*, v. 44, n. 7, pp. 2067–2079, 2003.
- [20] Kim, J., Moon, T.J., Howell, J.R., “Cure Kinetic Model, Heat of Reaction, and Glass Transition Temperature of AS4/3501–6 Graphite–Epoxy Prepregs”, *Journal of Composite Materials*, v. 36, n. 21, pp. 2479–2498, 2015.
- [21] Zhang, G., Wang, J., Ni, A., “Process-Induced Stress and Deformation of Variable-Stiffness Composite Cylinders During Curing”, *Materials*, v. 12, n. 2, pp. 1–14, 2019.
- [22] Krishnan, A., Conway, A., Xiao, X., “Assessment of a Progressive Fatigue Damage Model for AS4/3501–6 Carbon Fiber/Epoxy Composites Using Digital Image Correlation”, *Applied Composite Materials*, v. 26, n. 15, pp. 1227–1246, 2019.
- [23] Kim, Y.K., White, S.R., “Stress relaxation behavior of 3501–6 epoxy resin during cure”, *Polymer Engineering & Science*, v. 36, n. 23, pp. 2852–2862, 2010.